Synchronization of Plant Circadian Oscillators with a Phase Delay Effect of the Vein Network

Hirokazu Fukuda,[1,*] Norihito Nakamichi,[2] Mihoe Hisatsune,[1] Haruhiko Murase,[1] and Takeshi Mizuno[2]

[1]*Department of Applied Life Sciences, Graduate School of Life and Environmental Sciences, Osaka Prefecture University, Sakai 599-8531, Japan*

[2]*Laboratory of Molecular Microbiology, School of Agriculture, Nagoya University, Chikusa-ku, Nagoya, 464-8601 Japan*

(Received 11 January 2007; published 29 August 2007)

Synchronization phenomena in coupled circadian oscillators of plant leaves were investigated experimentally using bioluminescence technology for a clock gene. Analyzing the phase of circadian oscillation, the phase-wave propagations and the phase delay caused by the vein network were observed. We describe these phase dynamics using a two-layer model with coupled Stuart-Landau equations. Global synchronization of circadian oscillators in the leaf is also investigated.

DOI: 10.1103/PhysRevLett.99.098102 PACS numbers: 87.19.Jj, 05.45.Xt

Introduction.—Synchronization phenomena in numerous coupled oscillators have been studied in physical, chemical, and biological systems [1–3]. These spatiotemporal dynamics underlie many important activities of living organisms to maintain life, e.g., heart contraction and circadian rhythms. Complex networks of biological oscillators produce both biological rhythms. Recently, complex and heterogeneous networks of connections among oscillators have been shown to play an important role in physiological processes. A grid network of ventricular fibrillation can eliminate cardiac arrhythmia related to spiral waves in excitable media [4]. Entrainment mediated by direct photic inputs from eyes to the suprachiasmatic nucleus, which adapts mammals' circadian rhythms to periodic daily variation, is dependent on the topology of the connection among circadian oscillating neurons [5].

In plants, the circadian oscillator system also has complex and heterogeneous oscillator networks. Nearly all cells in plants show self-sustained circadian oscillation, which is generated through expression of clock genes [6]. The plant cells mutually couple via the diffusion of materials in two major connections: plasmodesmata and vascular bundles (called *veins* in the leaf) [7,8]. Plasmodesmata directly connect nearest-neighbor cells [9]. In contrast, vascular bundles spread over the whole plant to transport materials among all tissues quickly [8]. Plasmodesmata and vascular bundles, respectively, produce nearest-neighbor coupling and the long-range coupling. Physiologically, plant cells can also couple through short-range, extracellular signaling as well as through plasmodesmata. Moreover, the cells inside vascular bundles in the mature stage cannot generate circadian oscillation themselves because they have no nucleus which holds the clock genes [8]. Consequently, the cells inside the vascular bundle are inactive cells for circadian oscillation. Therefore, the plant circadian oscillator system comprises local-coupled active oscillators and the long-range-coupled inactive elements. For that reason, the plant circadian oscillator system might show various dynamics such as those in a partially aging oscillator system [10] and nonlocally coupled oscillator systems [11,12]. Previous studies have revealed that the spatiotemporal waves occur in the leaf [13] and the coupling of plant circadian oscillators is so weak that resynchronization between phase-inverted regions in a leaf progresses very slowly [14]. However, the details of such synchronization phenomena of coupled plant circadian oscillators have not been clarified yet. In this Letter, we describe experimental investigation of the dynamics of the plant circadian oscillator system.

Materials and methods.—Our experiments are carried out using the transgenic *Arabidopsis thaliana* (Columbia accession, Col) *CCA1::LUC* whose clock gene *CCA1* is fused to a modified firefly luciferase gene [15]. The *CCA1::LUC* plants are grown on agar Murashige and Skoog plant salt mixture medium with 2% (w/v) sucrose, containing 8 μg/ml of luciferin [16] under continuous white light (80 μmol m^{-2} s^{-1}) at 22 $\pm$ 1 °C for 20 d. Before 24 h from the start of monitoring of bioluminescence, 8 mg/ml luciferin was sprayed on plants or detached leaves. The bioluminescence intensity is proportional to the expression rate of *CCA1*. We measured bioluminescence using a highly sensitive CCD camera (VIM Camera C2741-35A; Hamamatsu Photonics KK, Japan) in the dark at 22 $\pm$ 1 °C.

Results and discussions.—Figures 1(a) and 1(d), respectively, show images of the bioluminescence of an intact plant and a detached leaf. Almost all plant cells emitted bioluminescence rhythmically, indicating that the clock gene *CCA1* is expressed in almost all cells periodically. The average period of oscillation in both the intact plant and the detached leaf was about 25 h. In the intact plant, however, the period of oscillation often depended on the organ unexpectedly [Fig. 1(b)]. In the center of the rosette [point A in Fig. 1(a)], the period of oscillations was about 24 h. In contrast, in the center of a leaf [point B in Fig. 1(a)], the period was about 35 h. Such period differences among organs depend on individuals [Fig. 1(c)]. In the intact plant, Fig. 1(b) shows that the magnitudes of the amplitude of oscillations remained roughly constant after a large damping at the first oscillation. On the other hand, in the detached leaf, the period of the oscillations remained

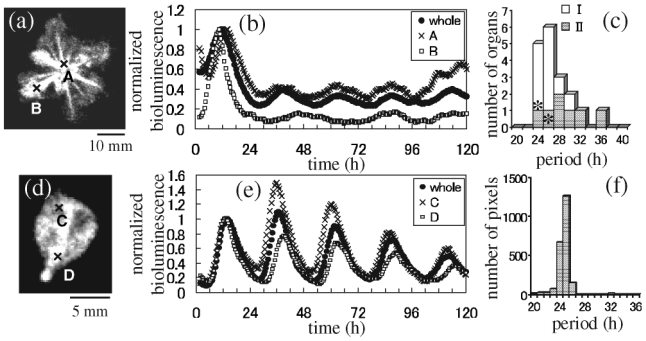

FIG. 1. Circadian rhythms of intact plant (a)–(c) and detached leaf (d)–(f) under continuous dark. (a),(d) Images of bioluminescence. (b),(e) Time series of intensity of bioluminescence. (c) Distribution of period of organs in two intact plants I and II. The asterisk indicates the period of the center of each rosette. (f) Distribution of the period of pixels in five detached leaves.

approximately constant over the leaf [Fig. 1(e)]. The distribution of period of pixels in five detached leaves shows a sharp peak at 25 h [Fig. 1(f)]. The detached leaf maintained the magnitude of amplitudes better than the intact plant [17]. In both systems, however, the circadian oscillation was damped with time under continuous dark.

To characterize the synchronization of circadian oscillators, we introduce the phase ϕ of the oscillators [2],

$$\phi(t) = 2\pi \frac{t - \tau_k}{\tau_{k+1} - \tau_k}, \tag{1}$$

where τ_k is the time of the kth peak of the oscillatory time series of pixels in bioluminescence images, and $\tau_k \leq t < \tau_{k+1}$. Figure 2 shows the circadian oscillations' phase in each pixel of bioluminescence images in both the leaf of the intact plant and the detached leaf. In both leaves, phase-wave propagations were observed. In the intact leaf, the phase waves propagated simultaneously from several starting points that were distributed throughout the leaf [Fig. 2(a)]. In the detached leaf, the phase waves propagated from a few points scattered over the leaf [Fig. 2(b)].

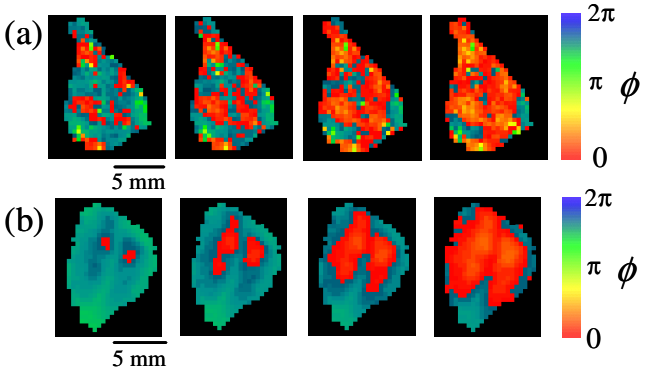

FIG. 2 (color online). Time evolution of the phase ϕ of the circadian oscillations in leaves: leaf of an intact plant (a) and detached leaf (b). The time interval between images is 1 h. The areas of detached leaves increased by 7% per day, and no correction was made for this growth.

This difference of phase-wave propagations between the intact and detached leaves might result from the difference of the velocity of diffusion in their vein because transportation with high velocity in veins might be abandoned by leaf detachment. The phase-wave propagation velocity was about 3 mm/h in all cases for both the intact and detached leaves in our experiment. This velocity indicates that these phase waves are traveling waves resulting from the diffusion of materials among cells.

Except for a few leaves, nearly detached leaves showed regular traveling waves. Figure 3 shows a spiral wave on the detached leaf. A core of the spiral wave is visible on vertical line A in Fig. 3(b). To investigate the phase and amplitude profile on the core, they were plotted as shown, respectively, in Figs. 3(c) and 3(d). On the core, the phase ϕ changed discontinuity and the amplitude of oscillation became low, indicating that this core has features of the singular point. Consequently, the plant circadian oscillators can produce a spiral wave with a singular point similarly to oscillating Ginzburg-Landau media [1].

Next, we investigate the effect of the vein network for the phase dynamics on the leaf. Figure 4(a) shows that the vein structure emerges from the image of phase ϕ in the detached leaf. The phase delay was observed on the vein tissue maximally at 0.5π. To elucidate this phenomenon, we consider a two-layer model using the coupled Stuart-Landau equations [12] as follows:

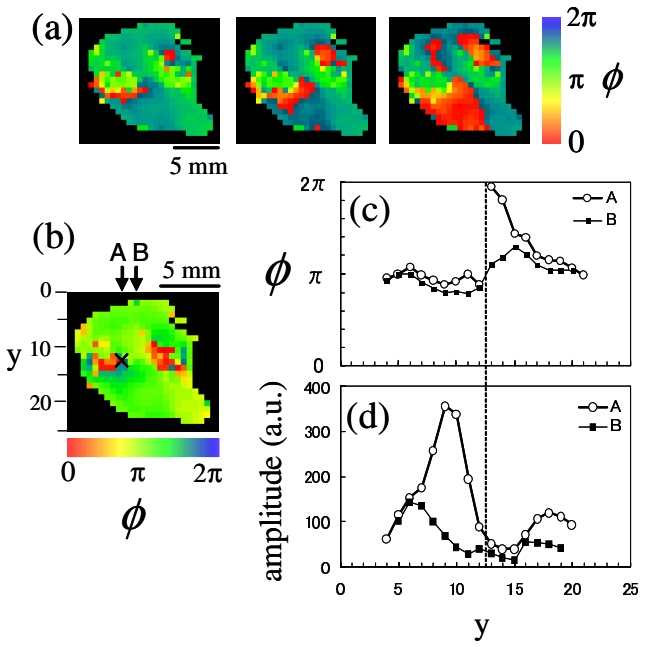

FIG. 3 (color online). Spiral wave on the detached leaf. (a) Time evolution of the phase ϕ of the circadian oscillations in the detached leaf. The time interval between two images is 2 h. In (b), the cross indicates a core of the spiral wave. (c) Radial profile for phase ϕ on both vertical lines A and B in (b). (d) Radial profile for the amplitude on both vertical lines A and B in (b). The broken line indicates the position of the core of the spiral wave.

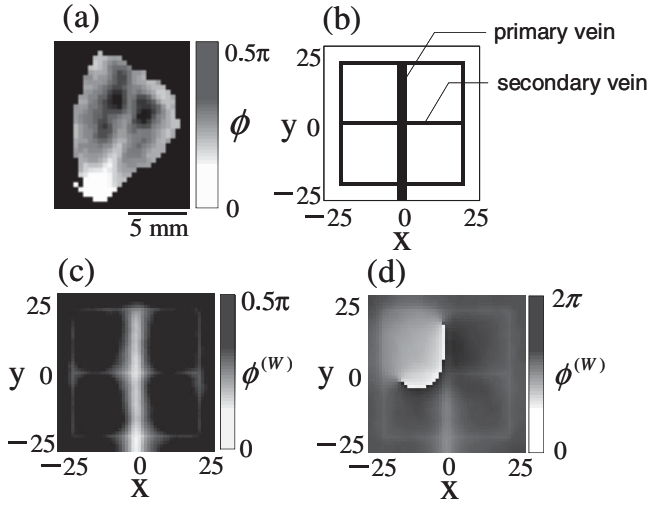

FIG. 4. (a) Vein structure emerged from the image of phase ϕ in the detached leaf. (b) Architecture of a vein network of the secondary layer in our numerical simulations. A three-pixel-wide line on $x = 0$ and a one-pixel-wide grid line, respectively, show the primary vein and the secondary vein. (c),(d) Phase $\phi^{(W)}$ of oscillation from numerical simulation. The coupling constants are $K_p = K_{pv} = K_v = 1$.

$$\frac{dW_k}{dt} = (\alpha + i\omega_k - |W_k|^2)W_k + K_p\sum_{\langle l\rangle}(W_l - W_k) + K_{pv}(Z_k - W_k), \quad (2)$$

$$\frac{dZ_k}{dt} = \beta Z_k + K_v\sum_{\langle l\rangle}(Z_l - Z_k) + K_{pv}(W_k - Z_k). \quad (3)$$

In those equations, $W_k = A_k^{(W)}\exp(i\phi_k^{(W)})$ is the complex amplitude of the kth oscillator on the first layer, and $Z_k = A_k^{(Z)}\exp(i\phi_k^{(Z)})$ is the complex amplitude of the kth oscillator on the secondary layer. Active cells such as epidermal and mesophyll cells form the first layer. Figure 4(b) shows that the secondary layer is a grid network of inactive cells which construct the vein in the mature stage [7]. The cells inside the mature vein cannot produce the circadian oscillations themselves because they have no clock genes. In addition, $\alpha(>0)$ is a parameter specifying the distance from a Hopf bifurcation, ω_k is the natural frequency of an active cell k and is distributed uniformly in a finite range $[\omega_0 - \Delta\omega, \omega_0 + \Delta\omega]$, $\beta(<0)$ is a parameter indicating the magnitude of the decay of Z_k. The active cells and inactive cells are coupled with their nearest neighbors via diffusion. Furthermore, K_p is the coupling constant between active cells via diffusion through plasmodesmata, K_v is the coupling constant between inactive cells via diffusion through the holes between vein cells, and K_{pv} is the coupling constant between active cells and inactive cells via diffusion through plasmodesmata. In the intact leaf, it seems that $K_p \sim K_{pv} \ll K_v$. On the other hand, in the detached leaf, K_v might take a smaller value than in an intact plant because high-velocity transportation in veins might be eliminated by leaf detachment. The summation over the nearest neighbors of the cell k is denoted by $\Sigma_{\langle l\rangle}$. The boundary condition is the Neumann boundary condition. Numerical simulations were performed using the fourth-order Runge-Kutta method. In this Letter, the parameter values are denoted as $\alpha = 1$, $\beta = -0.3$, $\omega_0 = 1$, and $\Delta\omega = 0.1$.

Figure 4(c) shows the vein structure on the image of $\phi^{(W)}$ obtained by numerical simulation from a completely synchronized initial condition. A phase delay of $\phi^{(W)}$ on the vein network was observed. In this case, the maximum phase delay was about 0.5π. This phase delay effect can be observed regardless of the value of K_v [see the insets of Fig. 6(b)]. Figure 4(d) shows spiral waves in $\phi^{(W)}$ obtained using a numerical simulation with a certain initial condition: both $\phi^{(W)}$ and $\phi^{(Z)}$ of a fifth part area in the top left were changed in the opposite phase, indicating that the spiral waves might be generated easily on the leaf by starting from partially inverted initial conditions.

We now discuss the synchronization rate R for circadian oscillators in the leaf defined as

$$Re^{i\Phi} = \frac{1}{N}\sum_{k=1}^{N} e^{i\phi_k}, \quad (4)$$

where ϕ_k is the phase of oscillator k, N is the total number of oscillators. Figure 5 shows R as a function of time. In the detached leaves that showed the traveling waves, as shown in Fig. 2(b), R maintained a high value ($R \sim 0.9$). In the detached leaf that showed the spiral phase wave (Fig. 3), R maintained a mediate value ($R \sim 0.6$). In the numerical simulation of the detached leaf arranged as Fig. 4(b), R depends on the initial conditions. From the completely

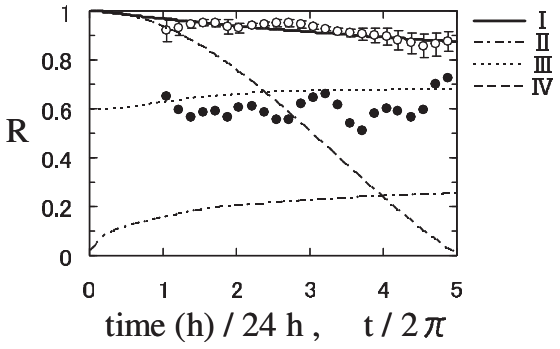

FIG. 5. Synchronization rate R as a function of time. The open circles indicate the average of R of five detached leaves, which show the traveling waves as Fig. 2(b). The error bars indicate the standard deviation. The closed circles indicate R of a detached leaf, which shows the spiral wave as shown in Fig. 3. Lines I–III are obtained from numerical simulations with different initial conditions for $\phi^{(W)}$ and $\phi^{(Z)}$: I, completely synchronized initial conditions; II, random initial conditions; and III, partially inverted initial conditions as Fig. 4(d). The coupling constants are $K_p = K_{pv} = K_v = 1$. Line IV is obtained using numerical simulations with a completely synchronized initial condition and $K_p = K_{pv} = K_v = 0$.

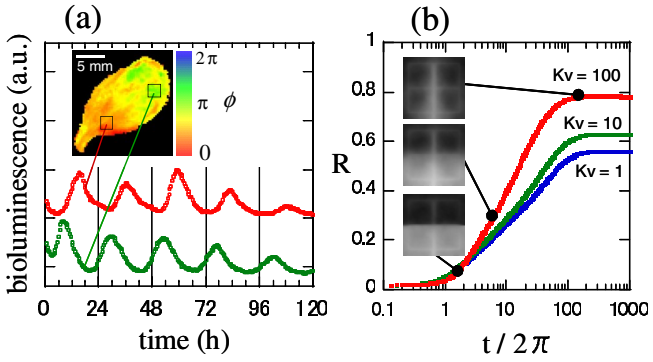

FIG. 6 (color online). (a) Resynchronization process between almost phase-inverted regions in a detached leaf under continuous dark. To create the phase-inverted regions, after the leaf was detached, two inverted 12 h light, 12 h dark cycles were given to the detached leaf during 2 d using foil covers as Ref. [14]. The inset shows the phase ϕ at 17 h. (b) Synchronization rate R during resynchronization process between phase-inverted regions in a leaf obtained from numerical simulations. The insets show images of the phase $\phi^{(W)}$ using the same gray scale as that used for Fig. 4(d). The coupling constants are $K_p = K_{pv} = 1$.

synchronized initial conditions (I in Fig. 5), R retains a high value ($R \sim 0.9$). The phase-wave propagations and the phase delay effect by the vein network occur in this case. From random initial conditions (II in Fig. 5) and partially inverted initial conditions (III in Fig. 5), the spiral waves occur and R maintains lower values. Restraint for R is caused by stationary spiral waves on the leaf.

The resynchronization process between phase-inverted regions in a detached leaf has also been investigated [Fig. 6(a)]. For 120 h, the difference of peak time of oscillations between distal and proximal regions decreased from 7.5 to 5.5 h, indicating that the resynchronization progressed slowly as a previous work [14]. We have measured this resynchronization process with six detached leaves, four leaves in them gave similar results. The numerical simulations were performed using models (2) and (3) to estimate the necessary time for completion of resynchronization. Figure 6(b) shows that the estimated time for resynchronization between the leaf halves was about 200π (equal to 100 circadian cycles). Results also revealed that R at the stationary state increased with K_v, indicating that the high-velocity transportation in the vein network contributes to improvement of global synchronization.

Conclusions.—We have identified phase-wave propagations in coupled circadian oscillators of plant leaves using bioluminescence technology for a clock gene. The traveling wave patterns, including spiral wave, were observed. It is especially interesting that the vein network, inactive cells network, produces the phase delay of circadian oscillation. These phenomena can be described in a two-layer model using the coupled Stuart-Landau equations. In addition, the synchronization of circadian oscillators in leaves was investigated. The vein network often has a nested grid structure, but this study addressed only primary and secondary vein structures. Probably, the higher microscopic structures of vein influence the phase dynamics of circadian oscillators, especially when the diffusion constant of veins differs greatly from that of plasmodesmata. Further elucidation of details is now in progress.

We are grateful to Professor H. Daido of Osaka Prefecture University for helpful discussions. N. N. was supported by the Japan Society for the Promotion of Science (Grant No. 18006334). T. M. was supported by a Grant-in-Aid from the Ministry of Education, Culture, Sports, Science, and Technology of Japan.

*fukuda@bioinfo.osakafu-u.ac.jp

[1] Y. Kuramoto, *Chemical Oscillations, Waves, and Turbulence* (Springer, Berlin, 1984).
[2] H. Fukuda, H. Morimura, and S. Kai, Physica (Amsterdam) **205D**, 80 (2005).
[3] A. Pikovsky, M. Rosenblum, and J. Kurths, *Synchronization—A Universal Concept in Nonlinear Sciences* (Cambridge University Press, Cambridge, U.K., 2001); I. Z. Kiss, Y. Zhai, and J. L. Hudson, Science **296**, 1676 (2002); H. Fukuda, N. Tamari, H. Morimura, and S. Kai, J. Phys. Chem. A **109**, 11 250 (2005); A. T. Winfree, *The Geometry of Biological Time* (Springer, New York, 2001).
[4] H. Sakaguchi and Y. Kido, Phys. Rev. E **71**, 052901 (2005).
[5] H. Kori and A. S. Mikhailov, Phys. Rev. Lett. **93**, 254101 (2004).
[6] C. R. McClung, The Plant Cell **18**, 792 (2006); J. C. W. Locke, A. J. Millar, and M. S. Turner, J. Theor. Biol. **234**, 383 (2005); H. Fukuda, J. Kodama, and S. Kai, BioSystems **77**, 41 (2004).
[7] S. Turner and L. E. Sieburth, *The Arabidopsis Book* (American Society of Plant Biologists, Washington, DC, 2003), DOI: 10.1199/tab.0073, see http://www.aspb.org/publications/arabidopsis/.
[8] U. Ludewig and W. B. Frommer, *The Arabidopsis Book* (American Society of Plant Biologists, Washington, DC, 2002), DOI: 10.1199/tab.0092, see http://www.aspb.org/publications/arabidopsis/.
[9] B. Ding, Plant Mol. Biol. **38**, 279 (1998).
[10] H. Daido and K. Nakanishi, Phys. Rev. Lett. **93**, 104101 (2004).
[11] S. Shima and Y. Kuramoto, Phys. Rev. E **69**, 036213 (2004).
[12] V. Casagrande and A. S. Mikhailov, Physica (Amsterdam) **205D**, 154 (2005).
[13] U. Rascher, M.-T. Hütt, K. Siebke, B. Osmond, F. Beck, and U. Lüttge, Proc. Natl. Acad. Sci. U.S.A. **98**, 11 801 (2001).
[14] S. C. Thain, A. Hall, and A. J. Millar, Curr. Biol. **10**, 951 (2000).
[15] N. Nakamichi, S. Ito, T. Oyama, T. Yamashino, T. Kondo, and T. Mizuno, Plant Cell Physiol. **45**, 57 (2004).
[16] N. Nakamichi, M. Kita, S. Ito, T. Yamashino, and T. Mizuno, Plant Cell Physiol. **46**, 686 (2005).
[17] A. Hall, L. Kozma-Bognár, R. Tóth, F. Nagy, and A. J. Millar, Plant Physiol. **127**, 1808 (2001).